

straint fits. In the case of invisible spectator protons, before entering the fitting procedure a momentum of zero was assigned to the spectator. The momentum had errors $P_x = P_y = 30$ MeV/c and $P_z = 40$ MeV/c. Once again the fit is a seven-constraint fit, this technique being the accepted one for reproducing the expected momentum distribution using the Fourier transform of the Hulthén wave function. The resolution for the invisible spectator events is only slightly worse than for the seen spectator events and does not affect the analysis.

⁶Our detection efficiency for events with unseen spectator was slightly less than for the seen spectator. This was so particularly for those events with small laboratory angle between the K^- and the π^- . A 4% correction was made to account for the screening effect.

⁷Our center-of mass energy E^* of the K^-n system covers the range $2.7 \lesssim E^* \lesssim 3.3$ because of the Fermi motion of the neutron. The backward hyperon events did not seem to come from any narrow resonance in this energy region.

⁸J. S. Loos, V. E. Kruse, and E. L. Goldwasser, Phys. Rev. **173**, 1330 (1968).

⁹O. I. Dahl, L. M. Hardy, R. L. Hess, J. Kirz, D. H. Miller, and J. A. Schwartz, Phys. Rev. **163**, 1430

(1968).

¹⁰D. J. Crennell, G. R. Kalbfleisch, K. W. Lai, J. M. Scarr, T. G. Schumann, I. O. Skillicorn, and M. S. Webster, Phys. Rev. Letters **18**, 86 (1967).

¹¹The reaction $\pi^- p \rightarrow \Lambda^0 K^0$ has $B = 7.5 \pm 2.0$ at 5 GeV/c. J. Weisbach, Purdue University, private communication.

¹²J. D. Jackson, Rev. Mod. Phys. **37**, 484 (1965; J. D. Jackson, J. T. Donohue, K. Gottfried, R. Keyser, and B. E. Y. Svensson, Phys. Rev. **139**, B428 (1965).

¹³A. H. Rosenfeld, N. Barash-Schmidt, A. Barbaro-Galtieri, L. R. Price, P. Söding, C. G. Wohl, M. Roos, and W. J. Willis, Rev. Mod. Phys. **40**, 77 (1968).

¹⁴R. R. Kofler, R. W. Hartung, and D. D. Reeder, Phys. Rev. **163**, 1479 (1967).

¹⁵The polarization in the reaction $\pi^- p \rightarrow \Lambda^0 K^0$ changes sign at $-t \sim 0.5$ (GeV/c)² at an incident momentum near 4 GeV/c (Ref. 9). There is evidence that this is still so at 5 GeV/c (Ref. 11), but at 6 GeV/c the polarization is consistent with zero for $-t < 0.5$ (Ref. 10).

¹⁶D. D. Reeder and K. V. L. Sarma, Phys. Rev. **172**, 1566 (1968).

¹⁷M. P. Locher and H. Romer, Phys. Letters **23**, 496 (1966).

¹⁸R. C. Arnold, Phys. Rev. **153**, 1506 (1967).

PRODUCTION OF K_2^0 MESONS AND NEUTRONS BY 10- AND 16-GeV ELECTRONS ON BERYLLIUM*

A. D. Brody, W. B. Johnson, D. W. G. S. Leith, G. Loew, J. S. Loos, G. Luste, R. Miller, K. Moriyasu, B. C. Shen, W. M. Smart, and R. Yamartino
Stanford Linear Accelerator Center, Stanford University, Stanford, California 94305
(Received 13 March 1969)

We have measured the K_2^0 yields for electron energies of 10 and 16 GeV and at production angles of 2° and 4°, using a 40-in. hydrogen bubble chamber as a K_2^0 detector. The observed yields are compared with the predictions of a model involving the intermediate photoproduction of $\varphi(1020)$ mesons. In addition, we have measured the relative neutron-to- K_2^0 ratio as a function of the secondary beam momentum.

The yields of strongly interacting charged particles produced in electron-Be collisions have been measured recently at the Stanford Linear Accelerator Center (SLAC) by several groups¹⁻⁴ and confirm the general features of the calculations made by Tsai⁵ and others. We report here a measurement of the K_2^0 yields from Be for electron energies of 10 and 16 GeV and production angles of 2° and 4°. The SLAC 40-in. hydrogen bubble chamber was used as the K_2^0 decay detector. The observed K_2^0 yields are consistent with the average of K^+ and K^- yields reported previously.^{1,2,4} A comparison with the K_2^0 yields expected from the photoproduction of $\varphi(1020)$ mesons indicates that this process alone cannot explain either the observed magnitude or the angular dependence of the data. A preliminary mea-

surement of the intensity and momentum spectrum of neutrons at the chamber indicates that favorable K_2^0 -to-neutron ratios may be obtained for secondary beam momenta above 2 GeV/c.

The primary electron beam from the accelerator was focused on a Be target which was mounted downstream of a vertical bending magnet. This magnet allowed variation of the production angle of the neutral beam within the range 1.5°-5°. The intensity of the electron beam was measured by use of a toroid charge integrator. The position and focus of the electron beam at the target were continuously monitored by a closed circuit television display of a ruled ZnS sheet attached to the upstream end of the Be target. The neutral beam passed through a sweeping magnet to clear out charged particles, a γ -ray

filter,⁶ and the defining collimator. This collimator was a 1.2-m Pb block placed 10 m downstream from the Be target and had an angular acceptance of $12.5 \mu\text{sr}$. Additional sweeping magnets and shadowing collimators (nondefining) were located along the beam path to the bubble chamber which was situated 56 m downstream of the target.

The intensity and momentum spectrum of the K_2^0 mesons at the chamber are simply related to the momentum distributions of the charged particles from the three-body K_2^0 decays in flight. In a method similar to that used by Firestone⁷ and Hopkins, Bacon, and Eisler⁸ we measured the momenta of the positive particle (\vec{P}_+) and the negative particle (\vec{P}_-) and tabulated the quantity P_{vis} , defined as $|\vec{P}_+| + |\vec{P}_-|$. Using Monte Carlo methods we then generated the expected P_{vis} distributions for each decay mode, corresponding to small intervals of incident K_2^0 momentum. Since the decay mode of individual events was not determined, the expected P_{vis} distributions were summed over the three charged decay modes (K_{e3} , $K_{\mu3}$, and $K_{\pi3}$) in proportion to their established rates.⁹ Finally, the incident K_2^0 momentum spectrum was iterated until the observed P_{vis} distribution could be reproduced satisfactorily. The resulting K_2^0 momentum spectra, within the statistical accuracy of this experiment, were completely insensitive to the parameters of the K_2^0 decays.¹⁰

Identification of K_2^0 decays and measurement of the quantity P_{vis} were done at the scan table. A physicist examined every recorded decay for acceptability; care was taken to eliminate electron pairs and decays associated with interactions in the chamber or in the entrance window. Subsequent precision measurement and spatial reconstruction of 100 accepted events indicated that the final sample contained $\sim 6\%$ non- K_2^0 decays. The measurement of P_{vis} was done using a circle template at the scan table since the method does not require high precision on individual measurements. A comparison with the 100 reconstructed events showed that individual template values of P_{vis} were accurate to within $\pm 10\%$.

Momentum spectra at the chamber were determined for 2° and 4° production angles, for 10- and 16-GeV electrons incident on a 1.75-radiation-length (r.l.) Be target. Two multiplicative factors were then applied to extrapolate the K_2^0 yields to the target; the first was the reciprocal of the probability that the K_2^0 will reach the chamber before decaying,⁹ and the second was the

attenuation factor of the beam in the thick γ -ray filter.⁶ The attenuation factor for lead was measured by placing an additional 130 g/cm^2 of lead in the beam and repeating the measurement of the P_{vis} spectrum at 2° for 16-GeV electrons. The shapes of the P_{vis} distributions for the two measurements were the same within statistical uncertainties; the absolute flux was reduced by a factor of 2.4 with the additional lead. The attenuation for tungsten was extrapolated from lead, and that for lithium hydride was estimated from K -nucleon cross sections¹¹ and from K^\pm -Be cross sections at $3.5 \text{ GeV}/c$.¹² The overall attenuation factor was 16 ± 5 .¹³

In Table I and in Fig. 1, we present the measured K_2^0 yields, corrected for K_2^0 decay and for

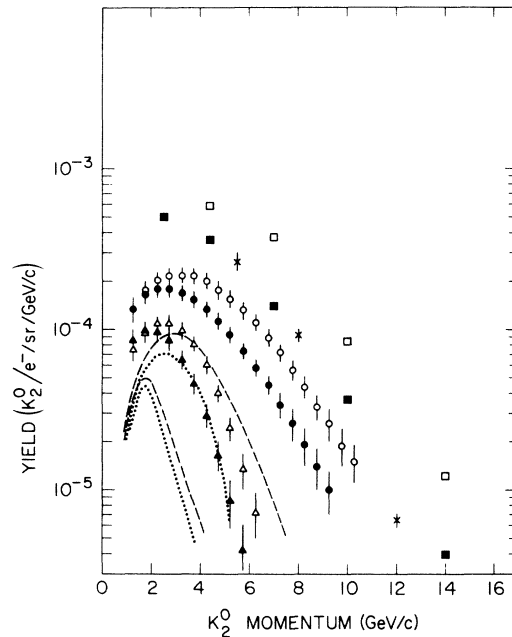


FIG. 1. Yields of K_2^0 mesons from a 1.75-r.l. Be target measured for the following electron energies and production angles: (open circles) 16 GeV, 2° ; (closed circles) 16 GeV, 4° ; (open triangles) 10 GeV, 2° ; and (closed triangles) 10 GeV, 4° . Shown for comparison are the average of K^+ and K^- yields previously measured under the following conditions: (crosses) 0° production with 16-GeV electrons on a 1.8-r.l. Be target (Ref. 1); (open squares) 1° production and (closed squares) 3° production with 18-GeV electrons on an 0.3-r.l. Be target (Ref. 2). The measurements of Ref. 2 have been extrapolated from 0.3- to 1.75-r.l. Be target. Predicted contributions from $\phi(1020)$ photoproduction are shown for the following electron energies and production angles: 16 GeV, 2° (upper dashed curve); 16 GeV, 4° (lower dashed curve); 10 GeV, 2° (upper dotted curve); and 10 GeV, 4° (lower dotted curve).

Table I. K_2^0 yields.

Electron Energy, GeV	10		16	
	2°	4°	2°	4°
Production Angle				
No. Events in P_{vis} Distribution	930	717	877	931
K_2^0 Momentum Interval, GeV/c	Yield ^a at Target $K_2^0/e^-/sr/\text{GeV}/c \times 10^{-4}$			
1.0 - 1.5	0.74 ± 0.12	0.85 ± 0.15	1.35 ± 0.24	1.35 ± 0.23
1.5 - 2.0	0.96 ± 0.14	0.97 ± 0.13	1.75 ± 0.24	1.67 ± 0.22
2.0 - 2.5	1.10 ± 0.12	0.96 ± 0.13	2.02 ± 0.24	1.80 ± 0.21
2.5 - 3.0	1.10 ± 0.12	0.85 ± 0.11	2.17 ± 0.24	1.78 ± 0.19
3.0 - 3.5	0.99 ± 0.11	0.65 ± 0.09	2.18 ± 0.23	1.68 ± 0.18
3.5 - 4.0	0.82 ± 0.09	0.46 ± 0.07	2.14 ± 0.23	1.54 ± 0.17
4.0 - 4.5	0.60 ± 0.08	0.29 ± 0.05	2.00 ± 0.22	1.35 ± 0.15
4.5 - 5.0	0.40 ± 0.05	0.17 ± 0.04	1.78 ± 0.21	1.13 ± 0.12
5.0 - 5.5	0.24 ± 0.04	0.09 ± 0.03	1.55 ± 0.19	0.93 ± 0.10
5.5 - 6.0	0.13 ± 0.03		1.31 ± 0.16	0.74 ± 0.08
6.0 - 6.5	0.07 ± 0.03		1.10 ± 0.13	0.58 ± 0.07
6.5 - 7.0			0.89 ± 0.12	0.45 ± 0.06
7.0 - 7.5			0.72 ± 0.09	0.34 ± 0.06
7.5 - 8.0			0.56 ± 0.08	0.26 ± 0.06
8.0 - 8.5			0.44 ± 0.07	0.19 ± 0.05
8.5 - 9.0			0.33 ± 0.06	0.14 ± 0.04
9.0 - 9.5			0.26 ± 0.06	
9.5 - 10.0			0.19 ± 0.05	
10.0 - 10.5			0.15 ± 0.04	

^aErrors quoted do not include the overall uncertainty of ±35% (see text).

beam attenuation. The uncertainties given include both statistical fluctuations and estimates for possible differences in relative normalization between the four spectra. The systematic uncertainty in attenuation (±35%) applies to all four spectra together and is not included in the table.

For comparison, the average of K^+ and K^- yields are also shown in Fig. 1. The 0° data of Barna et al.¹ (for 16-GeV electrons on a 1.8-r.l. Be target) agree very well with our yields. The data of Boyarski et al.² at 1° and 3° (for 18-GeV electrons on a 0.3-r.l. Be target) have been extrapolated to a 1.75-r.l. Be target,¹⁴ and are consistent with our yields.

Yield estimates made by Tsai⁵ indicate that the most important single process for K_2^0 production is photoproduction of $\phi(1020)$ mesons which subsequently decay via $K_1^0 K_2^0$. However, many other processes may contribute, such as $K^*(890)$ photoproduction, two-body or quasi two-body processes (e.g., $\gamma N \rightarrow K^0 Y$), or production by interactions of secondary pions within the target. To determine the relative importance of $\phi(1020)$ photopro-

duction, we have calculated expected K_2^0 yields¹⁵ for this process for our electron energies and production angles. The results of the calculations are shown in Fig. 1 as dashed lines for 16-GeV electrons and as dotted lines for 10-GeV electrons. The magnitudes of the ϕ model curves are lower than our data, but more important, the drastic angular dependence predicted by the model is in contradiction to our experimental observations. Thus, we conclude that other processes are very important in K_2^0 production.

A preliminary measurement of the relative flux of neutrons to K_2^0 mesons at the chamber has been made. The ratio of the total number of K_2^0 mesons to the total number of neutrons incident at the chamber has been determined by a total interaction count. Denoting the neutron-to- K_2^0 ratio by R , one has

$$R = [(N_{\text{tot}} - N_K)/\sigma_n] (N_K/\sigma_K)^{-1},$$

where N_{tot} is the total number of interactions, N_K the number of expected K_2^0 induced interactions, and σ_K and σ_n the $K_2^0 p$ and $n p$ total cross sections,¹⁶ respectively. The following values for R were found: at 10 GeV,

$$8.5 \pm 1.7 \text{ at } 2^\circ,$$

and

$$9.9 \pm 2.0 \text{ at } 4^\circ;$$

at 16 GeV,

$$3.5 \pm 0.6 \text{ at } 2^\circ,$$

and

$$4.0 \pm 0.6 \text{ at } 4^\circ.$$

However, due to the strong momentum dependence of the neutron momentum distribution (shown below), only ~10% of the neutrons have momenta greater than 2 GeV/c.

A preliminary neutron momentum spectrum was measured from an analysis of three-pronged interactions in the chamber. In this case, the neutral beam was produced at 2° by 16-GeV electrons incident on an 0.9-r.l. Be target. From this sample, 403 events were found which fitted the three-constraint hypothesis,

$$n p \rightarrow p p \pi^-.$$

The momentum distribution of neutrons at the chamber, presented in Fig. 2, was obtained by dividing the number of events observed in each momentum interval by the cross section $\sigma(n p \rightarrow p p \pi^-)$.¹⁷ Also shown in Fig. 2 is the corre-

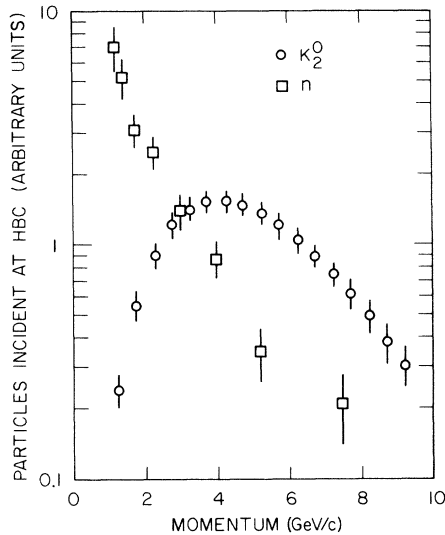


FIG. 2. Comparison of the neutron and K_2^0 fluxes at the hydrogen bubble chamber for 2° production with 16-GeV electrons.

sponding K_2^0 spectrum at the chamber.¹⁸ The relative normalization of the K_2^0 and neutron distributions is accurate to within 40%. As seen in Fig. 2, the neutron momentum spectrum at the chamber peaks below 1.0 GeV/c and the neutron-to- K_2^0 ratio decreases by an order of magnitude over the neutral-beam momentum range from 2 to 5 GeV/c.

We wish to thank A. Kilert, W. Walsh, R. Friday, D. McShurley, and A. Baumgarten for help in design and construction of the neutral beam, R. Watt and the bubble chamber staff, and our scanning and measuring staff. We are grateful for several discussions with Y. S. Tsai.

*Work supported by the U. S. Atomic Energy Commission.

¹A. Barna et al., Phys. Rev. Letters **18**, 360 (1967).

²A. M. Boyarski et al., in "Stanford Linear Accelerator Center Users Handbook," Stanford University, Stanford, Calif., Revised, 1968 (unpublished).

³A. Boyarski et al., Phys. Rev. Letters **18**, 363 (1967).

⁴Stanley M. Flatté et al., Phys. Rev. Letters **18**, 366 (1967).

⁵Y. S. Tsai, in "Stanford Linear Accelerator Center Users Handbook," Stanford University, Stanford, Calif. 1966 (unpublished). References to previous work are given in this paper.

⁶The γ filter consisted of 147 g/cm² of tungsten, 173 g/cm² of lead, and 50 g/cm² of lithium hydride.

⁷A. Firestone, thesis, Yale University, 1967 (unpublished).

⁸H. W. K. Hopkins, T. C. Bacon, and F. R. Eisler, Phys. Rev. Letters **19**, 185 (1967).

⁹All K_2^0 parameters used were taken from the compilation of the Particle Data Group, University of California Radiation Laboratory Report No. 8030, Revised, 1968 (to be published).

¹⁰The analysis was done using the values 0, 0.022, and -0.25 for ξ and λ (parameters of the leptonic decays) and A (parameter for the $\pi^+\pi^-\pi^0$ decay), respectively. Then the analysis was repeated using simple phase space for all decay modes. The K_2^0 spectra resulting from the two analyses agreed well within statistical uncertainties.

¹¹V. Cook et al., Phys. Rev. Letters **7**, 182 (1961); V. Cook et al., Phys. Rev. **123**, 320 (1961); A. N. Diddens, E. W. Jenkins, T. F. Kycia, and K. F. Riley, Phys. Rev. Letters **10**, 262 (1963); W. Galbraith et al., Phys. Rev. **138**, B913 (1965).

¹²W. V. Hassenzahl, thesis, University of Illinois, 1967 (unpublished).

¹³This $\pm 35\%$ systematic uncertainty in attenuation completely dominates the systematic uncertainties due to solid angle or charge integration.

¹⁴These extrapolations have been made from curves given in Ref. 5 and have normalization uncertainties of 20 to 40%.

¹⁵Our calculation is identical to that made by Y. S. Tsai et al., Phys. Rev. Letters **19**, 915 (1967), with the exceptions that (1) the $\varphi(1020)$ decays into $K_1^0K_2^0$ rather than into K^+K^- , and (2) the slope in t of the incoherent differential cross section is taken to be 5 (GeV/c)⁻² rather than 10 (GeV/c)⁻², as indicated by the recent $\varphi(1020)$ photoproduction data of W. G. Jones et al., Phys. Rev. Letters **21**, 586 (1968).

¹⁶Values for $\sigma(K_2^0p)$ and $\sigma(np)$ were taken to be 20 and 38 mb, respectively.

¹⁷Measured values of $\sigma(np \rightarrow pp\pi^-)$ do not appear in the literature. Below 2.5 GeV/c, we have used the relation $\sigma(np \rightarrow pp\pi^-) = \frac{1}{2}\sigma(pp \rightarrow pp\pi^0)$ expected from the one-pion-exchange model with $I = \frac{3}{2}$ dominance at the pion-nucleon scattering vertex. Above 2.5 GeV/c, we have used the relation $\sigma(np \rightarrow pp\pi^-) = \sigma(\bar{p}p \rightarrow \bar{n}p\pi^-)$ expected from the one-pion-exchange model. Values for $\sigma(pp \rightarrow pp\pi^0)$ were taken from A. F. Dunaitsev and Y. D. Prokoshkin, Zh. Eksperim. i Teor. Fiz. **36**, 1656 (1959) [translation: Soviet Phys.-JETP **36**, 1179 (1959)]; D. V. Bugg et al., Phys. Rev. **133**, B1017 (1964); K. R. Chapman et al., Phys. Letters **11**, 253 (1964); and F. F. Chen et al., Phys. Rev. **103**, 211 (1956). Values for $\sigma(\bar{p}p \rightarrow \bar{n}p\pi^-)$ were taken from T. Ferbel et al., Phys. Rev. **137**, B1250 (1965); H. C. Dehne et al., Phys. Rev. **136**, B843 (1964); K. Böckmann et al., Nuovo Cimento **42A**, 954 (1966); and T. Ferbel, J. A. Johnson, H. L. Kraybill, J. Sandweiss, and H. D. Taft, Phys. Rev. **173**, 1307 (1968).

¹⁸The K_2^0 spectrum at 2° for 16-GeV electrons has been extrapolated from 1.75 to 0.9 r.l. Be, using the curves given in Ref. 5.

¹⁹The normalization of the neutron spectrum was determined by measuring R to be 3.2 ± 0.8 for the 0.9-r.l. data.